DYSTONIA

TYPE Brief Research Report
PUBLISHED 10 February 2026
DOI 10.3389/dyst.2026.14631

OPEN ACCESS

EDITED BY
G. W. Gant Luxton,
University of California, Davis,
United States

*CORRESPONDENCE
Yuqing Li,
yuqing.li@neurology.ufl.edu

†PRESENT ADDRESS
Ariel Luz Walker,
Center for Translational Research in Neurodegenerative Disease, University of Florida, Gainesville, FL, United States; McKnight Brain Institute, Department of Neuroscience, University of Florida, Gainesville, FL, United States

RECEIVED 16 March 2025
REVISED 11 December 2025
ACCEPTED 27 January 2026
PUBLISHED 10 February 2026

CITATION
Liu Y, Xing H, Yokoi F, Walker AL, Chen D, Rodriguez-Lebron E and Li Y (2026) Validation of a torsinA cerebellar knockdown model of DYT1 dystonia. *Dystonia* 5:14631.
doi: 10.3389/dyst.2026.14631

Validation of a torsinA cerebellar knockdown model of DYT1 dystonia

Yuning Liu[1,2], Hong Xing[1], Fumiaki Yokoi[1], Ariel Luz Walker[1†], Duo Chen[1], Edgardo Rodriguez-Lebron[3] and Yuqing Li[1*]

[1]Department of Neurology, Norman Fixel Institute for Neurological Diseases, McKnight Brain Institute, College of Medicine, University of Florida, Gainesville, FL, United States, [2]College of Biological Science and Technology, Beijing Forestry University, Beijing, China, [3]Department of Pharmacology and Therapeutics, College of Medicine, University of Florida, Gainesville, FL, United States

Dystonia is a movement disorder characterized by sustained or intermittent muscle contractions causing abnormal, often repetitive, movements, postures, or both. DYT1 dystonia is an early-onset dystonia caused by *DYT1/TOR1A* gene mutations with reduced penetrance. It is believed that dystonia is produced by abnormal brain networks, but details remain unknown. Recent studies have shown that acute cerebellar knockdown of torsinA using small hairpin RNAs (shRNAs) can induce overt dystonia in adult mice. However, shRNAs have off-target effects that may alter the expression of unintended genes. To avoid this issue, we generated an alternate acute torsinA knockdown model using cre-loxP technology by injecting AAV-*cre* into the cerebellum of the *Dyt1*$^{loxP/loxP}$ mouse. These knockdown mice exhibited overt dystonia and displayed a spinning behavior, characterized by bidirectional circling or spinning during tail suspension. The overt dystonia and spin behavior were not observed in control mice injected with the AAV-GFP virus. Additionally, the knockdown mice showed decreased spontaneous firing and reduced intrinsic excitability of Purkinje cells. These findings confirmed that the acute cerebellar knockdown of torsinA can produce overt dystonia and further support the cerebellum's role in the pathogenesis of DYT1 dystonia. However, the emergence of a spinning phenotype raises questions about the validity of the acute knockdown models as accurate representations of human dystonia.

KEYWORDS

AAV, cerebellum, DYT1 dystonia, Purkinje cell, torsinA

Introduction

Dystonia is a neurological disorder characterized by sustained or intermittent muscle contractions that result in abnormal, often repetitive movements, postures, or both [1]. DYT1 or DYT-TOR1A dystonia is the most common early-onset generalized dystonia [2]. Most patients carry a heterozygous three-nucleotide (Δ*GAG*) deletion in exon 5 of the *DYT1/TOR1A* gene, leading to the loss of a glutamate residue in the torsinA protein [3]. Although numerous studies suggest that this mutation results in a loss-of-function of torsinA, a toxic-gain-of-function effect cannot be ruled out [4, 5]. Nevertheless, the

precise mechanism by which the mutation leads to dystonia remains largely unknown. *Dyt1* knockin mice harboring the corresponding in-frame *ΔGAG* deletion in the endogenous *Dyt1/Tor1a* gene have been developed to mimic the human condition [6, 7]. Although these mice exhibit several dystonia-like phenotypes, such as motor and sensory deficits, abnormal gait, and hind limb muscle co-contraction [7–10], the lack of overt dystonia phenotypes in most genetically modified models has hindered progress in understanding the disease [11–17].

The cerebellum—and specifically its Purkinje cells—plays a key role in controlling movement and posture, with multiple animal studies implicating these cells in dystonia pathogenesis [15, 18–29]. *Dyt1* knockin mice show altered Purkinje cell morphology [30, 31] and abnormal firing patterns, with increased large-conductance calcium-activated potassium (BK) current and elevated BK channel protein levels [32]. Most importantly, acute knockdown of torsinA in the adult cerebellum using shRNAs induces overt dystonia in adult mice—an effect not observed when knockdown is performed during development or directed to the striatum [33], suggesting the likely involvement of cerebellar dysfunction in the pathogenesis of DYT1 and other dystonias.

The present study aims to validate cerebellar acute torsinA knockdown models of DYT1 dystonia. Small hairpin RNAs (shRNAs) or small interfering RNAs (siRNAs) are known to cause significant off-target effects that may alter the expression of unintended genes [34]. Here, we developed an alternate acute torsinA knockdown (AAV-cre KD) mouse model by bilateral stereotaxic injection of AAV5-CMV-cre-GFP into the cerebellum of $Dyt1^{loxP/loxP}$ mice, with wild-type (WT) mice receiving AAV5-CMV-GFP as controls. Cre-mediated recombination subsequently reduced torsinA expression in the cerebellum. The motor behavior of these mice and the electrophysiological properties of the cerebellar Purkinje cells were characterized.

Methods

Animal

$Dyt1^{loxP/loxP}$ mice were bred and genotyped as described previously [35, 36]. Genotyping for $Dyt1^{loxP/loxP}$ mice was performed by PCR using a set of Dyt1loxpF (5_-GAGGAG AAAATAGGGGCTCAGTAT-3_), Dyt1loxpR (5_-GAAGGT TGAGAAACTGCCTTAGAG-3_) primers for $Dyt1^{loxP}$. All experiments were carried out by investigators blind to the genotypes and treatment, in compliance with the USPHS Guide for Care and Use of Laboratory Animals, and approved by the IACUC at the University of Florida. The mice were housed with *ad libitum* access to food and water under 12 h light and 12 h dark.

Stereotaxic injection of AAV

AAV5-CMV-cre-GFP (#105545-AAV5) and AAV5-CMV-GFP (#105530-AAV5) were purchased directly from Addgene. Stereotaxic administration of AAV5-CMV-cre-GFP and AAV5-CMV-GFP was performed on 5- to 7-month-old male $Dyt1^{loxP/loxP}$ mice and WT mice under anesthesia using a mixture of O_2 and isoflurane (dosage 4% for induction, 1.5% maintenance), respectively. Mice received bilateral intracerebellar injections (two sites/hemisphere) of virus diluted in Lactated Ringer's solution (Hospira, Lake Forest, IL; four injections per cerebellum). For each injection, 2 μL volume was delivered to the medial or lateral cerebellar nucleus at a 0.1 μL/min infusion rate using a 10-μL Hamilton syringe (BD, Franklin Lakes, NJ) retrofitted with a glass micropipette. One minute after the infusion was completed, the micropipette was retracted 0.3 mm and allowed to remain in place for 4 min before complete removal from the mouse brain. Anterior-posterior and medial-lateral coordinates were calculated from the bregma, and the dorsal-ventral coordinates were calculated from the dural surface. These measurements were made on an experimentally determined flat skull, following the previously described protocol [37].

Immunohistrochemistry

Adult male WT mice injected with AAV-CMV-GFP were euthanized and perfused with ice-cold 0.1 M phosphate buffer (PB; pH 7.4) followed by 4% paraformaldehyde in 0.1 M phosphate-buffered saline (PBS; pH 7.4). The brains were incubated with the fixative overnight and then with 30% sucrose in 0.1 M PB until the brain sank. The brain was embedded in OCT medium, and sagittal sections (20 μm) were collected by a Cryostat Freezing Microtome.

The brain sections were washed three times in 10 mM glycine/0.1 M PB for 5 min each and blocked in 2% gelatin/0.1 M PB for 15 min, 10 mM glycine/0.1 M PB for 5 min, and 0.1% BSA/0.1 M PB for 5 min. The blocked slices were incubated in Anti-GFP chicken polyclonal primary antibody (GFP-1020, Aves Labs; 1:2500 dilution) in 1% BSA/0.1 M PB for 2 h and washed in 0.1% BSA/0.1 M PB for 5 min each, six times. The sections were then incubated with Alexa Fluor® 488 AffiniPure® Donkey Anti-Chicken IgY (IgG) (H + L) (Jackson ImmunoResearch, code no. 703-545-155, 1:800 Dilution) in 1% BSA/0.1 M PB for 2 h and then washed in 0.1% BSA/0.1 M PB for 5 min each, six times. The slices were mounted on glass slides using Vectashield Hard Set mounting medium for fluorescence (Vector Lab Inc., H-1000), covered with a cover glass, and stored at 4 °C overnight for subsequent imaging using a fluorescent microscope.

Images were acquired using a Keyence BZ-X810 fluorescence microscope equipped with a CCD detector. A ×4 objective lens

(numerical aperture 0.13; working distance 16.5 mm; plan field flatness) was used for imaging. Whole-section images were generated using the Keyence image-stitching program, and image analysis was performed with the BZ-X800 Analyzer software.

Western blot

Thirteen weeks after AAV injection, 7 AAV-injected *Dyt1*$^{loxP/loxP}$ mice and 3 *Dyt1*$^{loxP/loxP}$ control mice were euthanized, and the brains were harvested for Western blot as described [38]. Protein lysates were prepared and homogenized in an SDS-based lysis buffer. Samples were run on SDS-PAGE gel (BioRad) and transferred to Millipore Immobilon-FL PVDF membrane. Membranes were blocked and subsequently incubated with primary torsinA antibody (Abcam 34540, 1:300), β-tubulin (Santa Cruz sc-9935, 1:14,000) overnight, followed by the secondary antibody donkey anti-rabbit 680 (LICORbio 926-68073 1:15,000) or donkey anti-goat 800 CW (LICORbio 926-33214 1:15,000) for 2 h. After washing and drying the membranes, the signals were analyzed using LI-COR Odyssey imaging system.

Motor behavior assessment

The presence of dystonia and its severity were quantified using a previously published scale [33, 39]. Briefly, 0 = normal behavior; 1 = abnormal motor behavior, no dystonic postures; 2 = mild motor impairment, dystonic-like postures when disturbed; 3 = moderate impairment, frequent spontaneous dystonic postures; 4 = severe impairment, sustained dystonic postures. Seven AAV-injected *Dyt1*$^{loxP/loxP}$ mice and eight AAV-injected WT control mice were assessed by the dystonia scale at 3, 5, 7, 9, 11, and 13 weeks after injection, respectively. During routine handling in the later phase of the experiment, a severe spinning behavior was unexpectedly observed in a subset of KD mice. To characterize this emergent phenotype, the tail hang test [40] was performed and was systematically video-recorded just before euthanasia. These videos were subsequently analyzed frame by frame in a *post hoc* manner to quantify their features, including latency to onset, duration, and rotational speed (defined as rotations per second, RPS).

Electrophysiology

Thirteen weeks after AAV injection, 5 AAV-injected *Dyt1*$^{loxP/loxP}$ mice and 3 *Dyt1*$^{loxP/loxP}$ control mice were euthanized, and the brains were harvested for electrophysiology study. The brains were rapidly removed and briefly chilled in the ice-cold cutting solution containing (in mM) 180 sucrose, 2.5 KCl, 1.25 NaH_2PO_4, 25 $NaHCO_3$, 1 $CaCl_2$, 10 $MgCl_2$, and 10 D-glucose and were oxygenated with 95% O_2-5% CO_2 (pH 7.35~7.45). Parasagittal 300 μm-thick cerebellar brain slices were cut with a Vibratome (LEICA VT 1000S, Leica Microsystems, Wetzlar, Germany) in the same ice-cold cutting solution. Slices were first incubated on a brain slice keeper (AutoMate Scientific, Inc. Berkeley, CA) and covered by a thin layer of artificial cerebrospinal fluid (ACSF) containing (in mM) 126 NaCl, 2.5 KCl, 1.25 NaH_2PO_4, 25 $NaHCO_3$, 2 $CaCl_2$, 2 $MgCl_2$, and 10 D-glucose. They were constantly oxygenated at 35 °C for 60 min. After a minimum of 60 min of incubation, a slice was transferred to a submerged recording chamber with a continuous flow (1.5 mL/min) of oxygenated ACSF.

The spontaneous firing properties of the Purkinje cell were measured by cell-attached patch-clamp recording in brain slices as described [32, 41–45]. The Purkinje cells located in the apex and bank of the cerebellar vermis lobules 4 to 6 were identified by infrared visualization in parasagittal cerebellar slices. Lobules 4 to 6 were selected because they receive inputs from the hind limbs. The spontaneous action potentials were recorded by the voltage clamp with cell-attached mode, infrared-differential interference contrast microscopy (IR-DIC) with video microscopy (Axioskop-FS; Carl Zeiss, Jena, Germany), a 40× water-immersion lens, and an Axopatch 1D amplifier (Axon Instruments, Foster City, CA). The patch electrodes had a resistance of 5–10 MΩ when filled with a K-gluconate-based intracellular solution containing (in mM): 112.5 K-gluconate, 4 NaCl, 17.5 KCl, 0.5 $CaCl_2$, 5 MgATP, 1 NaGTP, 5 EGTA, 10 HEPES, pH 7.2 (osmolality 270–280 mOsm/l). Positive pressure was applied to the patch electrode as it approached the Purkinje cell. Suction was applied to the electrode to create a seal (>5 GΩ) between the recording pipette and the cell membrane. Action potential current was recorded in the current-clamp mode that maintained an average of 0 pA holding current. To isolate the intrinsic activity, we added picrotoxin (10 μM), CGP55845 (1 μM), and kynurenic acid (5 mM) to the ACSF to block synaptic transmission.

The intrinsic activity was assessed by whole-cell recording. After breaking through the cell membrane, access resistance was maintained throughout at <25 MΩ. The action potential for the current step recording was triggered by depolarizing the current steps by 300 ms. All experiments were maintained at 35 °C ± 0.5 °C by adjusting the temperature of the bathing solution using Warner TC-344B Dual Automatic Temperature Controller (Warner Instruments, Holliston, MA). Cell-attached and whole-cell recordings were obtained from Purkinje cells using Axopatch 1D Amplifier (Molecular Devices). The recording data were acquired using pClamp 10 software, and the signals were filtered at 5 kHz and digitized at 10 kHz using a DigiData 1440 (Molecular Devices). Cell firing activity was further analyzed by the Mini Analysis Program (Synaptosoft).

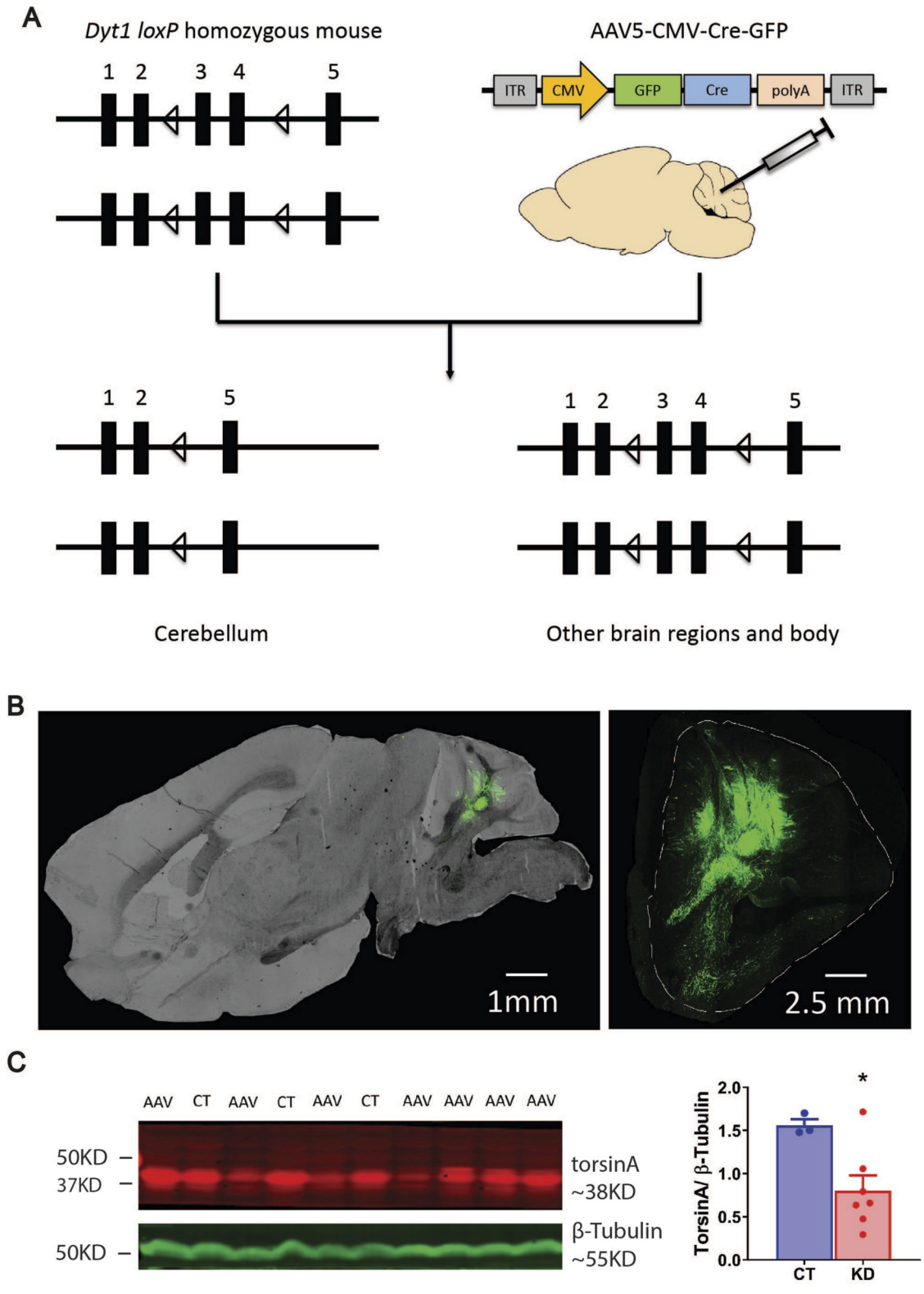

FIGURE 1
(A) Strategies to knock down torsinA in the cerebellum of adult mice using the *cre-loxP* system. Numbers represent the exons of the *Dyt1* or *Tor1a* gene, and the open triangles indicate *loxP* sequences inserted into the introns. **(B)** Strong GFP expression was observed in the cerebellum of the WT mice injected with AAV5-CMV-GFP. Sagittal sections were displayed. The left image was captured with a Keyence BZ-X810 microscope using
(*Continued*)

FIGURE 1 (Continued)
both regular and fluorescent lights and merged together. The stitched image on the right was captured by a Leica confocal microscope, and the contour of the cerebellum is outlined. **(C)** TorsinA protein expression levels were reduced in AAV-*cre* KD mice. Western blot and quantification showing a reduction in torsinA expression in cerebellar lysates from AAV-injected animals (AAV) compared to control mice (CT). Molecular marker locations are indicated on the left. TorsinA KD was reduced by 51% ± 11% (Mean ± S.E.M, torsinA KD n = 7; control n = 3). *$p < 0.05$.

Statistics

The Western blot signals were analyzed using the Student's t-test. Electrophysiological recording data were analyzed using the SAS/STAT mixed model for normally distributed data or GENMOD procedures when they were not normally distributed, with a log link for gamma distribution and a GEE model for repeated measurements. The statistical power was estimated using 1,000 simulations with a similar GENMOD model. The recorded neurons were nested within each animal. The age was used as a covariate in all electrophysiological analyses. Dystonia scores were evaluated using the SAS GENMOD procedure with a multinomial distribution, a cumulative logit link function, and a GEE model for repeated measurement. Significance was assigned at $p \leq 0.05$.

Results

The strategies used to knock down torsinA in the cerebellum are shown in Figure 1A. Instead of shRNA targeting torsinA mRNA, we took advantage of the cre-loxP system and the floxed *Dyt1* locus we developed earlier [35]. We used an AAV virus expressing Cre and GFP under the control of a general promoter, CMV. GFP was included to assess the efficiency of AAV transduction. Under UV light, strong fluorescent signals were observed in the cerebellum of AAV-injected mice (Figure 1B), confirming widespread AAV transduction. The effect of Cre-mediated recombination was assessed indirectly through a Western blot analysis of torsinA protein levels. Western blot showed a significant decrease in torsinA expression level in the cerebellar lysates of AAV-transduced animals compared to control mice (Figure 1C). In contrast, the levels in the cerebral cortex, brainstem, and striatum were unaffected (Supplementary Figure S1), suggesting successful inactivation of the endogenous *Dyt1* gene specifically in the cerebellum.

We observed the home cage behavior to determine whether the knockdown of torsinA resulted in overt dystonia (Supplementary Video S1). The presence of dystonia and its severity were assessed using a previously published Dystonia scale [33, 39]. Briefly, 0 = normal behavior; 1 = abnormal motor behavior, no dystonic postures; 2 = mild motor impairment, dystonic-like postures when disturbed; 3 = moderate impairment, frequent spontaneous dystonic postures; 4 = severe impairment, sustained dystonic postures. The KD mice showed overt dystonia in five out of seven mice within 9 weeks, as evidenced by abnormal hindlimb postures (Figure 2A) and increased overall dystonia scores in the KD mice ($\chi^2 = 7.55$, $p = 0.006$, Figure 2B). In addition to these general dystonic postures, a distinct and dramatic phenotype emerged in three of the five dystonic mice. This behavior was most clearly observed and captured on video during the later stages of the experiment, as the animals' general dystonia scores reached their peak severity. These mice exhibited recurrent episodes of vigorous, bidirectional spinning, particularly upon tail suspension (Supplementary Video S2). To provide a rigorous analysis, we quantified this behavior from the video recordings. The onset of spinning was remarkably rapid, with a latency of less than one second. The behavior was forceful and sustained; in the two most severely affected animals, the rotational speed reached up to 5.4 rotations per second (RPS), and the spinning bouts consistently lasted for more than 10 s. The third affected mouse displayed a similar but milder spinning phenotype. None of the WT control mice injected with an AAV5-CMV-GFP virus exhibited these phenotypes (Supplementary Videos S3, S4).

To contextualize these findings, we statistically compared the penetrance of overt dystonia in our AAV-cre KD model (71.4%, 5/7 mice) with established models. This penetrance rate is significantly higher than that reported in constitutive *Dyt1 ΔGAG* knock-in mice [6, 7], which typically exhibit no overt dystonia (0%; $p < 0.01$, Fisher's exact test). Furthermore, the high penetrance in our model is comparable to that observed in acute cerebellar shRNA knockdown models ($p > 0.05$) [33], supporting the validity of acute cerebellar suppression of torsinA in recapitulating motor symptoms.

To determine the effect of torsinA KD on Purkinje cell firing, we measured spontaneous firing and intrinsic excitability of the Purkinje cell in acute brain slices. Cell-attached recording of Purkinje cells revealed a 27% decrease in spontaneous firing frequency (control: 19 cells/3 mice; KD: 29 cells/5 mice; $p = 0.04$; statistical power = 1.0; Figures 3A,B) while coefficient of variation (CV) was not significantly altered ($p = 0.55$; Figure 3C). Decreased spontaneous firing in KD mice is consistent with our earlier finding in *Dyt1* knockin mice [32].

Depolarizing current steps were injected into the Purkinje cell of KD and control mice to assess intrinsic excitability. We injected a brief, positive current into the cell, which causes the membrane potential to become more positive, or depolarized. The action potentials produced are indicative of intrinsic excitability. KD mice exhibited 27% fewer action potentials than controls ($p = 0.0004$, Figures 3D–G). Decreased intrinsic

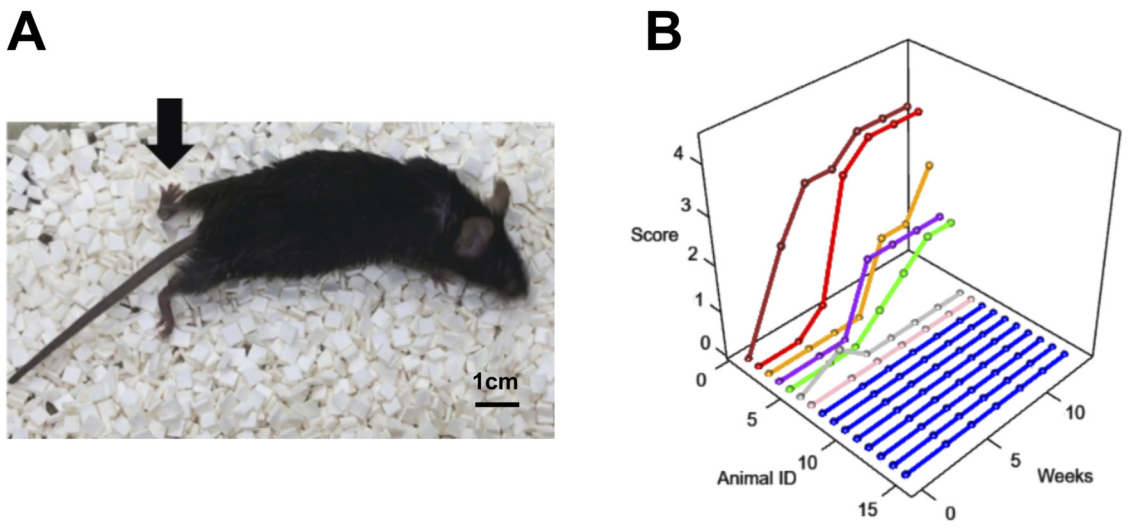

FIGURE 2
Overt dystonia phenotypes in AAV-cre KD mice. **(A)** Mouse #2 at 9 weeks after the injection of AAV-cre exhibited an abnormal hindlimb posture (arrow), scale bar = 1 cm. **(B)** The dystonia scores at 3, 5, 7, 9, 11, and 13 weeks after injections, and the injection day at 0 weeks are plotted for each AV-CMV-GFP-injected control mouse (blue; animal ID 8-15; n = 8) and AAV-CMV-Cre-GFP-injected KD mouse (other colors; animal ID 1-7; n = 7).

excitability indicated that the KD Purkinje cells would be less likely to fire action potentials, which could explain the decreased spontaneous firing frequency.

Discussion

We developed an alternate torsinA KD model to validate whether cerebellar torsinA KD can be a robust dystonia phenotypic model. Using the *cre-loxP* system-based approach, we observed overt dystonia in 5 out of 7 mice, similar to the shRNA KD model [33]. None of the 8 WT mice injected with AAV5-CMV-GFP showed overt dystonia, supporting that these symptoms are specific to torsinA knockdown rather than artifacts of the viral vector or surgery. *Dyt1* knockin mice show altered Purkinje cell morphology [30, 31] and abnormal spontaneous firing, with increased BK current and elevated BK channel protein levels [32]. BK channels have been implicated in dystonia [46–49]. Together, these results support a key role of the cerebellum in DYT1 dystonia. However, 3 of the 5 dystonic AAV-cre KD mice showed circling or spinning phenotype, which is not reported in the shRNA KD mice [33] and question the validity of cerebellar torsinA KD mice to model DYT1 dystonia.

Our KD mice and the previous shRNA KD mice show overt dystonia, supporting a key role of the cerebellum in DYT1 pathogenesis. In contrast, models with conditional torsinA knockout (pKO) or mutant knockin (Pcp2-KI) in Purkinje cells show better motor performance [50, 51]. The discrepancy may result from developmental compensation, as shRNA-mediated torsinA KD in young mice does not lead to overt dystonia [33]—or from the involvement of granule cells and deep cerebellum nuclei, which are affected in the KD models but spared in pKO and Pcp2-KI mice. Notably, during development, conditional knockin of *ΔGAG* mutation in the mouse cerebellum with engrailed1-Cre (En1 Cre) does not produce overt dystonia [4]. Future studies should use En1-creERT1 [52] or Pcp2-creERT2 [53] lines to inducibly knock out the *Dyt1* gene in adult mice to resolve these discrepancies.

Although both AAV-*cre* KD mice and shRNA KD mice support an essential role for the cerebellum in DYT1 pathogenesis, it remains unclear whether dystonia originates in the cerebellum. For example, Pcp2-KI mice showed normal Purkinje cell firing [41] in contrast to the global *Dyt1* knockin mice [32], suggesting that the cerebellum may act as a downstream node rather than the origin of dystonia. The Purkinje cell abnormality in *Dyt1* KI mice [32] likely originated from the striatum [41], and the overt dystonia in acute KD mice supports the idea that the cerebellum functions as a node downstream of the striatum via a disynaptic pathway linking these two structures [54]. Remarkably, conditional knockout of torsinA in the striatum mimics beam walking deficits in global *Dyt1* knockin mice [7, 36, 38], whereas acute shRNA KD in the adult striatum and globus pallidus does not produce overt dystonia [33]. The exact role of the cerebellum and basal ganglia in DYT1 dystonia remains to be fully delineated.

We found significantly reduced spontaneous firing *in vitro* in the AAV-*cre* KD mice, which is consistent with the *in vivo* finding from shRNA KD mice [33]. We examined further and

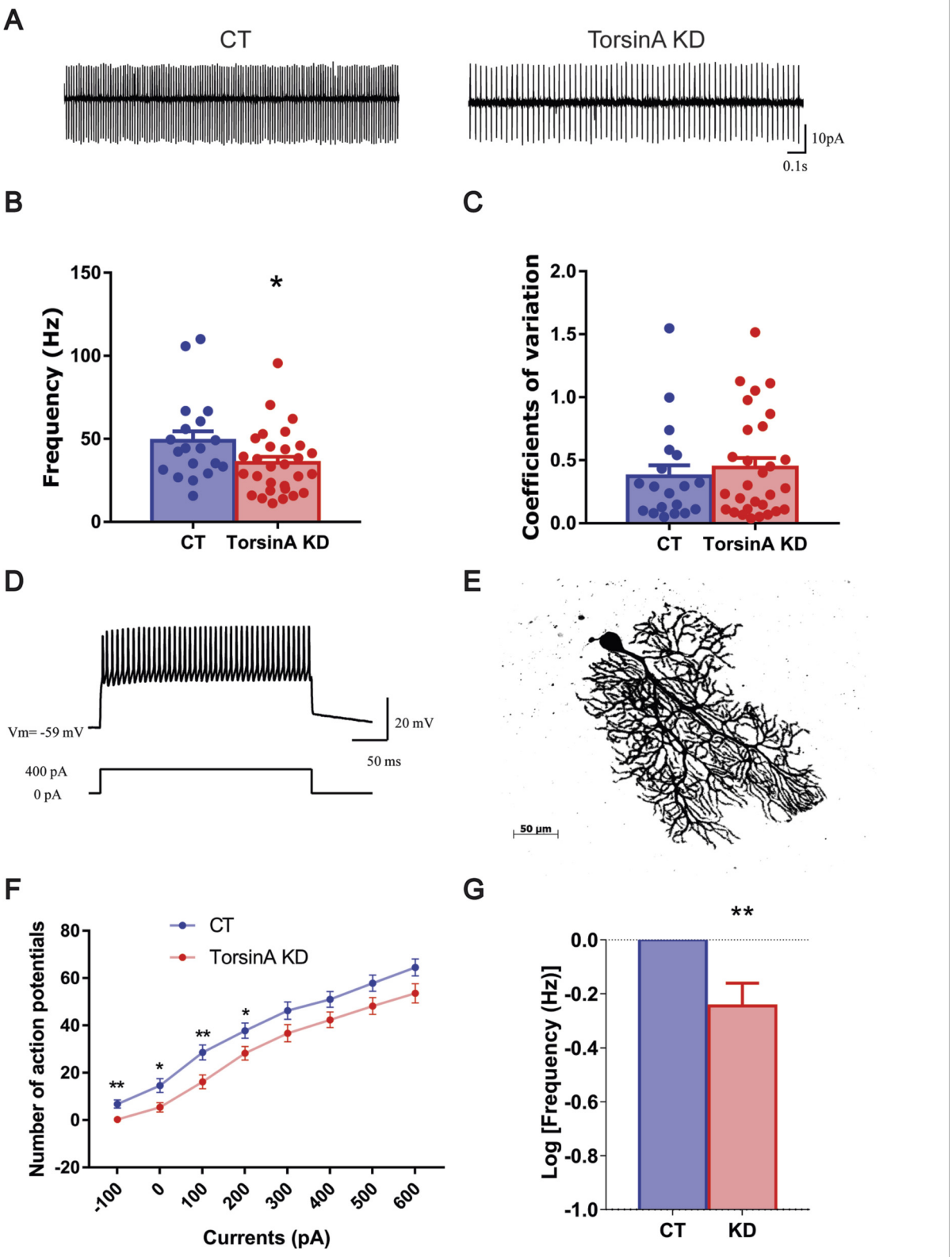

FIGURE 3
Decreased activity in Purkinje cells in AAV-*cre* KD mice was revealed by brain slice recording. **(A)** Representative traces for control and AAV-*cre* KD mice. **(B)** Comparison of the spontaneous firing frequency of Purkinje cells between AAV-*cre* KD and control mice. **(C)** Comparison of CV (coefficient of variation) of the Purkinje cells between control and AAV-*cre* KD mice. **(D)** Injected current-evoked action potentials of a recorded

(*Continued*)

FIGURE 3 (Continued)
Purkinje cell by the whole-cell recording mode. **(E)** The morphology of the recorded neuron was revealed by staining with biocytin/streptavidin Alexa Fluor 594 conjugate. Biocytin was included in the internal solution. **(F)** The frequency-current relationship for AAV-*cre* KD and control Purkinje cells. **(G)** In response to current-step stimulation, Purkinje cells fired 27% fewer action potentials in AAV-cre KD mice (20 cells/5 mice) than in the control mice (17 cells/3 mice). $*p < 0.05$, $**p < 0.01$, $***p < 0.001$.

found significantly decreased intrinsic excitability of AAV-*cre* KD Purkinje cells. Reduced intrinsic excitability would likely decrease the spontaneous firing of Purkinje cells both *in vivo* and *in vitro*. The molecular basis of reduced intrinsic excitability remains unknown, but we reported previously that BK channel activity was significantly increased [32], which could contribute to the decreased intrinsic excitability. Increased BK channel activity allows more potassium ions to move out of the cell, making the Purkinje cells less likely to fire. The AAV-cre KD mice are expected to reduce torsinA protein levels in other cerebellar neurons, including deep cerebellar nuclei, granule cells, and other interneurons. The effect of torsinA KD in these neurons remains to be investigated. Interestingly, aberrant outputs of glutamatergic neurons in deep cerebellar nuclei appear to mediate dystonic movement in the *Prrt2* mouse model [55], suggesting the importance of deep cerebellar nuclear neurons and their modulation by Purkinje cells.

We detected an unexpected bidirectional circling and spinning behavior during tail suspension in severely affected mice, resembling spinning behavior observed in a shRNA KD model targeting *Sgce* mRNA in the cerebellum, where motor deficits, spinning, and myoclonic-like jerky movements were alleviated by alcohol consumption [56]. The mutation of the *SGCE* gene causes myoclonus-dystonia or DYT11 dystonia [57]. The spinning behavior is unique to *Sgce* shRNA KD mice compared to other models of dystonia, including torsinA shRNA KD mice [56]. Although there is no spinning symptom in DYT11 dystonia patients, the alcohol rescue in the Sgce KD mice suggests that the spinning during tail suspension may be related to myoclonus-dystonia manifestation in mice, since DYT11 patients can get temporary relief by alcohol ingestion [58–60].

It is interesting that both *Sgce* shRNA KD and AAV-*cre* KD mice showed spinning behavior. ε-sarcoglycan, the product of the *Sgce* gene, is known to interact with torsinA. TorsinA binds to mutant ε-sarcoglycans and promotes their degradation [61]. Mutant mice with double mutations in the torsinA gene and *Sgce* show an earlier onset of motor deficits [62]. The common pathway affected in *Sgce* shRNA KD and AAV-*cre* KD mice remains to be determined.

On the other hand, vertigo, dizziness, and imbalance are associated with lesions of the vestibulo-cerebellar, vestibulo-spinal, or cerebellar ocular motor systems [63]. Acute knockdown of torsinA and *Sgce* might have damaged some of these systems, leading to the spinning behaviors in these mice. In the torsinA and *Sgce* KD mice without spinning behavior, it is plausible that vestibulo-cerebellar and cerebellar ocular motor system impairments exist, which may contribute to imbalance or even overt dystonia in torsinA and *Sgce* KD mice. Future research should explore localized or refined cerebellar AAV manipulations to avoid perturbations to the vestibulo-cerebellar and cerebellar ocular motor systems. It will also be interesting to study how vestibulo-cerebellar and cerebellar ocular motor system dysfunction contributes to dystonia pathogenesis and treatment. Vestibular dysfunction has been linked to focal or cervical dystonia [64–68]. A patient develops cervical dystonia soon after ear surgery that causes vestibular hypofunction [69]. Another report detailed an idiopathic cervical dystonia patient with benign paroxysmal positional vertigo [70]. To our knowledge, there are no reports of vestibular dysfunction in DYT1 and DYT11 dystonias, therefore, the acute torsinA and *Sgce* KD models may not accurately represent DYT1 and DYT11 dystonias. This is the major weakness of the current study and the use of acute gene KD models in dystonia research in general. Additionally, while our analysis of the spinning phenotype provided valuable data on its severity, a prospective study designed to systematically track the emergence and progression of this specific behavior from earlier time points would be necessary to understand its relationship with the overall dystonia pathology fully. Additional limitations include the fact that acute KD of torsinA in adults does not occur in DYT1 patients, and recent studies have pointed to a developmental origin of DYT1 dystonia [71–73]. This underscores the need for transgenic models with developmental genetic manipulations to replicate the human condition more accurately.

Data availability statement

The data supporting this study's findings are available from the corresponding author upon reasonable request.

Ethics statement

The animal study was approved by IACUC at the University of Florida. The study was conducted in accordance with the local legislation and institutional requirements.

Author contributions

YnL, ER-L, and YqL conceived and designed the study. YnL, HX, FY, AW, and ER-L gathered data. YnL and HX performed

statistical analyses. YnL and YqL wrote the article. All authors contributed to the article and approved the submitted version.

Funding

The author(s) declared that financial support was received for this work and/or its publication. Research reported in this publication was provided by Tyler's Hope for a Dystonia Cure and the Norman Fixel Institute for Neurological Diseases at UF Health, National Institutes of Health grants (NS75012, NS129873, AG087418). HX, FY, and YqL were partially supported by the Office of the Assistant Secretary of Defense for Health Affairs through the Peer-Reviewed Medical Research Program Discovery Award (W81XWH1810099 and W81XWH2110198).

Acknowledgements

We thank Caroline Comeau, Maisha Anika, Gracie Korkmaz, Shangru Lyu, Deepak Chhangani, Swapnil Pandey, and Qing-Shan Xue for their technical assistance and stimulating discussions.

Conflict of interest

The author(s) declared that this work was conducted in the absence of any commercial or financial relationships that could be construed as a potential conflict of interest.

Generative AI statement

The author(s) declared that generative AI was not used in the creation of this manuscript.

Any alternative text (alt text) provided alongside figures in this article has been generated by Frontiers with the support of artificial intelligence and reasonable efforts have been made to ensure accuracy, including review by the authors wherever possible. If you identify any issues, please contact us.

Author disclaimer

The content is solely the authors' responsibility and does not necessarily represent the official views of the National Institutes of Health. Opinions, interpretations, conclusions, and recommendations are those of the author and are not necessarily endorsed by the Department of Defense.

Supplementary material

The Supplementary Material for this article can be found online at: https://www.frontierspartnerships.org/articles/10.3389/dyst.2026.14631/full#supplementary-material

SUPPLEMENTARY FIGURE 1
TorsinA protein expression levels in the cerebral cortex, brainstem, and striatum were unaffected in AAV-*cre* KD mice. Western blot (images at the top) and quantification (bottom) showing no reduction in torsinA expression in cortical, brainstem, and striatal lysates from AAV-injected animals (KD) compared to control mice (CT, Mean ± S.E.M., torsinA KD n = 3; control n = 3).

References

1. Albanese A, Bhatia K, Bressman SB, DeLong MR, Fahn S, Fung VS, et al. Phenomenology and classification of dystonia: a consensus update. *Mov Disord* (2013) 28:863–73. doi:10.1002/mds.25475

2. Marras C, Lang A, van de Warrenburg BP, Sue CM, Tabrizi SJ, Bertram L, et al. Nomenclature of genetic movement disorders: recommendations of the international Parkinson and movement disorder society task force. *Mov Disord* (2016) 31:436–57. doi:10.1002/mds.26527

3. Ozelius LJ, Hewett JW, Page CE, Bressman SB, Kramer PL, Shalish C, et al. The early-onset torsion dystonia gene (DYT1) encodes an ATP-binding protein. *Nat Genetics* (1997) 17:40–8. doi:10.1038/ng0997-40

4. Weisheit CE, Dauer WT. A novel conditional knock-in approach defines molecular and circuit effects of the DYT1 dystonia mutation. *Hum Mol Genet* (2015) 24:6459–72. doi:10.1093/hmg/ddv355

5. Yokoi F, Chen H-X, Dang MT, Cheetham CC, Campbell SL, Roper SN, et al. Behavioral and electrophysiological characterization of Dyt1 heterozygous knockout mice. *Plos One* (2015) 10:e0120916. doi:10.1371/journal.pone.0120916

6. Goodchild RE, Kim CE, Dauer WT. Loss of the dystonia-associated protein TorsinA selectively disrupts the neuronal nuclear envelope. *Neuron* (2005) 48:923–32. doi:10.1016/j.neuron.2005.11.010

7. Dang MT, Yokoi F, McNaught KS, Jengelley TA, Jackson T, Li J, et al. Generation and characterization of Dyt1 DeltaGAG knock-in mouse as a model for early-onset dystonia. *Exp Neurol* (2005) 196:452–63. doi:10.1016/j.expneurol.2005.08.025

8. DeAndrade MP, Trongnetrpunya A, Yokoi F, Cheetham CC, Peng N, Wyss JM, et al. Electromyographic evidence in support of a knock-in mouse model of DYT1 dystonia. *Mov Disord* (2016) 31:1633–9. doi:10.1002/mds.26677

9. Song CH, Fan X, Exeter CJ, Hess EJ, Jinnah HA. Functional analysis of dopaminergic systems in a DYT1 knock-in mouse model of dystonia. *Neurobiol Dis* (2012) 48:66–78. doi:10.1016/j.nbd.2012.05.009

10. Richter F, Gerstenberger J, Bauer A, Liang CC, Richter A. Sensorimotor tests unmask a phenotype in the DYT1 knock-in mouse model of dystonia. *Behav Brain Res* (2017) 317:536–41. doi:10.1016/j.bbr.2016.10.028

11. Oleas J, Yokoi F, DeAndrade MP, Pisani A, Li Y. Engineering animal models of dystonia. *Mov Disord* (2013) 28:990–1000. doi:10.1002/mds.25583

12. Richter F, Richter A. Genetic animal models of dystonia: common features and diversities. *Prog Neurobiol* (2014) 121:91–113. doi:10.1016/j.pneurobio.2014.07.002

13. Tassone A, Sciamanna G, Bonsi P, Martella G, Pisani A. Experimental models of dystonia. *Int Rev Neurobiol* (2011) 98:551–72. doi:10.1016/B978-0-12-381328-2.00020-1

14. Dauer W, Goodchild R. Mouse models of torsinA dysfunction. *Adv Neurol* (2004) 94:67–72.

15. Rey Hipolito AG, van der Heijden ME, Sillitoe RV. Physiology of dystonia: animal studies. *Int Rev Neurobiol* (2023) 169:163–215. doi:10.1016/bs.irn.2023.05.004

16. El Atiallah I, Bonsi P, Tassone A, Martella G, Biella G, Castagno AN, et al. Synaptic dysfunction in dystonia: update from experimental models. *Curr Neuropharmacol* (2023) 21:2310–22. doi:10.2174/1570159X21666230718100156

17. Oleas J, Yokoi F, DeAndrade MP, Li Y (2015) LeDoux M (ed.), In *Movement disorders: genetics and models*. Academic Press, New York, pp. 483–505.

18. Bologna M, Berardelli A. The cerebellum and dystonia. *Handb Clin Neurol* (2018) 155:259–72. doi:10.1016/B978-0-444-64189-2.00017-2

19. Kaji R, Bhatia K, Graybiel AM. Pathogenesis of dystonia: is it of cerebellar or basal ganglia origin? *J Neurol Neurosurg Psychiatry* (2018) 89:488–92. doi:10.1136/jnnp-2017-316250

20. Shakkottai VG, Batla A, Bhatia K, Dauer WT, Dresel C, Niethammer M, et al. Current opinions and areas of consensus on the role of the cerebellum in dystonia. *Cerebellum* (2017) 16:577–94. doi:10.1007/s12311-016-0825-6

21. Tewari A, Fremont R, Khodakhah K. It's not just the basal ganglia: cerebellum as a target for dystonia therapeutics. *Mov Disord* (2017) 32:1537–45. doi:10.1002/mds.27123

22. Bologna M, Berardelli A. Cerebellum: an explanation for dystonia? *Cerebellum Ataxias* (2017) 4:6. doi:10.1186/s40673-017-0064-8

23. Prudente CN, Hess EJ, Jinnah HA. Dystonia as a network disorder: what is the role of the cerebellum? *Neuroscience* (2014) 260:23–35. doi:10.1016/j.neuroscience.2013.11.062

24. Filip P, Lungu OV, Bares M. Dystonia and the cerebellum: a new field of interest in movement disorders? *Clin Neurophysiol* (2013) 124:1269–76. doi:10.1016/j.clinph.2013.01.003

25. Sadnicka A, Hoffland BS, Bhatia KP, van de Warrenburg BP, Edwards MJ. The cerebellum in dystonia - help or hindrance? *Clin Neurophysiol* (2012) 123:65–70. doi:10.1016/j.clinph.2011.04.027

26. LeDoux MS. Animal models of dystonia: lessons from a mutant rat. *Neurobiol Dis* (2011) 42:152–61. doi:10.1016/j.nbd.2010.11.006

27. LeDoux MS, Lorden JF. Abnormal cerebellar output in the genetically dystonic rat. *Adv Neurol* (1998) 78:63–78.

28. Morigaki R, Miyamoto R, Matsuda T, Miyake K, Yamamoto N, Takagi Y. Dystonia and cerebellum: from bench to bedside. *Life (Basel)* (2021) 11:776. doi:10.3390/life11080776

29. Jackson NN, Stagray JA, Snell HD. Cerebellar contributions to dystonia: unraveling the role of Purkinje cells and cerebellar nuclei. *Dystonia* (2025) 4:14006. doi:10.3389/dyst.2025.14006

30. Zhang L, Yokoi F, Jin YH, DeAndrade MP, Hashimoto K, Standaert DG, et al. Altered dendritic morphology of Purkinje cells in Dyt1 DeltaGAG knock-in and purkinje cell-specific Dyt1 conditional knockout mice. *PLoS One* (2011) 6:e18357. doi:10.1371/journal.pone.0018357

31. Song CH, Bernhard D, Hess EJ, Jinnah HA. Subtle microstructural changes of the cerebellum in a knock-in mouse model of DYT1 dystonia. *Neurobiol Dis* (2014) 62:372–80. doi:10.1016/j.nbd.2013.10.003

32. Liu Y, Xing H, Wilkes B, Yokoi F, Chen H, Vaillancourt D, et al. The abnormal firing of Purkinje cells in the knockin mouse model of DYT1 dystonia. *Brain Research Bulletin* (2020) 165:14–22. doi:10.1016/j.brainresbull.2020.09.011

33. Fremont R, Tewari A, Angueyra C, Khodakhah K. A role for cerebellum in the hereditary dystonia DYT1. *Elife* (2017) 6:e22775. doi:10.7554/eLife.22775

34. Bereczki Z, Benczik B, Balogh OM, Marton S, Puhl E, Pétervári M, et al. Mitigating off-target effects of small RNAs: conventional approaches, network theory and artificial intelligence. *Br J Pharmacol* (2025) 182:340–79. doi:10.1111/bph.17302

35. Yokoi F, Dang MT, Mitsui S, Li J, Li Y. Motor deficits and hyperactivity in cerebral cortex-specific Dyt1 conditional knockout mice. *J Biochemistry* (2008) 143:39–47. doi:10.1093/jb/mvm191

36. Yokoi F, Dang MT, Li J, Standaert DG, Li Y. Motor deficits and decreased striatal dopamine receptor 2 binding activity in the striatum-specific Dyt1 conditional knockout mice. *Plos One* (2011) 6:e24539. doi:10.1371/journal.pone.0024539

37. Rodriguez-Lebron E, Costa Mdo C, Luna-Cancalon K, Peron TM, Fischer S, Boudreau RL, et al. Silencing mutant ATXN3 expression resolves molecular phenotypes in SCA3 transgenic mice. *Mol Ther* (2013) 21:1909–18. doi:10.1038/mt.2013.152

38. Yokoi F, Oleas J, Xing H, Liu Y, Dexter KM, Misztal C, et al. Decreased number of striatal cholinergic interneurons and motor deficits in dopamine receptor 2-expressing-cell-specific Dyt1 conditional knockout mice. *Neurobiol Dis* (2020) 134:104638. doi:10.1016/j.nbd.2019.104638

39. Calderon DP, Fremont R, Kraenzlin F, Khodakhah K. The neural substrates of rapid-onset Dystonia-Parkinsonism. *Nat Neurosci* (2011) 14:357–65. doi:10.1038/nn.2753

40. Pappas SS, Darr K, Holley SM, Cepeda C, Mabrouk OS, Wong JM, et al. Forebrain deletion of the dystonia protein torsinA causes dystonic-like movements and loss of striatal cholinergic neurons. *Elife* (2015) 4:e08352. doi:10.7554/eLife.08352

41. Xing H, Girdhar P, Liu Y, Yokoi F, Vaillancourt DE, Li Y. Subtle changes in Purkinje cell firing in Purkinje cell-specific Dyt1 ΔGAG knock-in mice. *Dystonia* (2025) 4:14148. doi:10.3389/dyst.2025.14148

42. Liu Y, Xing H, Ernst AF, Liu C, Maugee C, Yokoi F, et al. Hyperactivity of Purkinje cell and motor deficits in C9orf72 knockout mice. *Mol Cell Neurosci* (2022) 121:103756. doi:10.1016/j.mcn.2022.103756

43. Lyu S, Xing H, Liu Y, Girdhar P, Yokoi F, Li Y. Further studies on the role of BTBD9 in the cerebellum, sleep-like behaviors and the restless legs syndrome. *Neuroscience* (2022) 505:78–90. doi:10.1016/j.neuroscience.2022.10.008

44. Lyu S, Xing H, DeAndrade MP, Perez PD, Yokoi F, Febo M, et al. The role of BTBD9 in the cerebellum, sleep-like behaviors and the restless legs syndrome. *Neuroscience* (2020) 440:85–96. doi:10.1016/j.neuroscience.2020.05.021

45. Xing H, Girdhar P, Yokoi F, Li Y. Sex-specific alterations of Purkinje cell firing in Sgce knockout mice and correlations with myoclonus. *Dystonia* (2025) 4:14415. doi:10.3389/dyst.2025.14415

46. Lowe SA, Wilson AD, Aughey GN, Banerjee A, Goble T, Simon-Batsford N, et al. Modulation of a critical period for motor development in Drosophila by BK potassium channels. *Curr Biol* (2024) 34:3488–505.e3483. doi:10.1016/j.cub.2024.06.069

47. Buckley C, Williams J, Munteanu T, King M, Park SM, Meredith AL, et al. Status dystonicus, oculogyric crisis and paroxysmal Dyskinesia in a 25 year-old woman with a novel. *Tremor Other Hyperkinet Mov (N Y)* (2020) 10:49. doi:10.5334/tohm.549

48. Zhang G, Gibson RA, McDonald M, Liang P, Kang PW, Shi J, et al. A gain-of-function mutation in KCNMA1 causes dystonia spells controlled with stimulant therapy. *Mov Disord* (2020) 35:1868–73. doi:10.1002/mds.28138

49. Thomsen M, Ott F, Loens S, Kilic-Berkmen G, Tan AH, Lim SY, et al. *Genetic diversity and expanded phenotypes in dystonia: insights from large-scale exome sequencing* (2024). medRxiv.

50. Wilkes BJ, Adury RZ, Berryman D, Concepcion LR, Liu Y, Yokoi F, et al. Cell-specific Dyt1 ΔGAG knock-in to basal ganglia and cerebellum reveal differential effects on motor behavior and sensorimotor network function. *Exp Neurol* (2023) 367:114471. doi:10.1016/j.expneurol.2023.114471

51. Yokoi F, Dang MT, Li Y. Improved motor performance in Dyt1 Delta GAG heterozygous knock-in mice by cerebellar Purkinje-cell specific Dyt1 conditional knocking-out. *Behav Brain Res* (2012) 230:389–98. doi:10.1016/j.bbr.2012.02.029

52. Sgaier SK, Millet S, Villanueva MP, Berenshteyn F, Song C, Joyner AL. Morphogenetic and cellular movements that shape the mouse cerebellum; insights from genetic fate mapping. *Neuron* (2005) 45:27–40. doi:10.1016/j.neuron.2004.12.021

53. Korecki AJ, Hickmott JW, Lam SL, Dreolini L, Mathelier A, Baker O, et al. Twenty-Seven tamoxifen-inducible iCre-Driver mouse strains for eye and brain, including seventeen carrying a new inducible-first constitutive-ready allele. *Genetics* (2019) 211:1155–77. doi:10.1534/genetics.119.301984

54. Bostan AC, Strick PL. The basal ganglia and the cerebellum: nodes in an integrated network. *Nat Rev Neurosci* (2018) 19:338–50. doi:10.1038/s41583-018-0002-7

55. Wu XM, Lu B, He JY, Zhang YX, Wu ZY, Xiong ZQ. Aberrant outputs of glutamatergic neurons in deep cerebellar nuclei mediate dystonic movements. *Sci Adv* (2025) 11:eadp2377. doi:10.1126/sciadv.adp2377

56. Washburn S, Fremont R, Moreno-Escobar MC, Angueyra C, Khodakhah K. Acute cerebellar knockdown of Sgce reproduces salient features of myoclonus-dystonia (DYT11) in mice. *Elife* (2019) 8:e52101. doi:10.7554/eLife.52101

57. Zimprich A, Grabowski M, Asmus F, Naumann M, Berg D, Bertram M, et al. Mutations in the gene encoding epsilon-sarcoglycan cause myoclonus-dystonia syndrome. *Nat Genet* (2001) 29:66–9. doi:10.1038/ng709

58. Cazurro-Gutiérrez A, Marcé-Grau A, Correa-Vela M, Salazar A, Vanegas MI, Macaya A, et al. ε-Sarcoglycan: unraveling the myoclonus-dystonia gene. *Mol Neurobiol* (2021) 58:3938–52. doi:10.1007/s12035-021-02391-0

59. Roze E, Lang AE, Vidailhet M. Myoclonus-dystonia: classification, phenomenology, pathogenesis, and treatment. *Curr Opin Neurol* (2018) 31:484–90. doi:10.1097/WCO.0000000000000577

60. Weissbach A, Werner E, Bally JF, Tunc S, Löns S, Timmann D, et al. Alcohol improves cerebellar learning deficit in myoclonus-dystonia: a clinical and electrophysiological investigation. *Ann Neurol* (2017) 82:543–53. doi:10.1002/ana.25035

61. Esapa CT, Waite A, Locke M, Benson MA, Kraus M, McIlhinney RA, et al. SGCE missense mutations that cause myoclonus-dystonia syndrome impair epsilon-sarcoglycan trafficking to the plasma membrane: modulation by

ubiquitination and torsinA. *Hum Mol Genet* (2007) 16:327–42. doi:10.1093/hmg/ddl472

62. Yokoi F, Yang G, Li J, DeAndrade MP, Zhou T, Li Y. Earlier onset of motor deficits in mice with double mutations in Dyt1 and Sgce. *J Biochem* (2010) 148: 459–66. doi:10.1093/jb/mvq078

63. Bodranghien F, Bastian A, Casali C, Hallett M, Louis ED, Manto M, et al. Consensus paper: revisiting the symptoms and signs of cerebellar syndrome. *Cerebellum* (2016) 15:369–91. doi:10.1007/s12311-015-0687-3

64. Kukurin G. Targeting sensory systems in the treatment of dystonia: outcomes from a case series. *Med Res Arch* (2024) 12. doi:10.18103/mra.v12i6.5447

65. Guha A, Agharazi H, Gupta P, Shaikh AG. Exploring heading direction perception in cervical dystonia, tremor, and their coexistence. *Brain Sci* (2024) 14: 217. doi:10.3390/brainsci14030217

66. Agharazi H, Wang A, Guha A, Gupta P, Shaikh AG. Unraveling the twist: spatial navigational challenges in cervical dystonia. *Mov Disord* (2023) 38:2116–21. doi:10.1002/mds.29612

67. Sarasso E, Emedoli D, Gardoni A, Zenere L, Canu E, Basaia S, et al. Cervical motion alterations and brain functional connectivity in cervical dystonia. *Parkinsonism Relat Disord* (2024) 120:106015. doi:10.1016/j.parkreldis.2024.106015

68. Münchau A, Bronstein AM. Role of the vestibular system in the pathophysiology of spasmodic torticollis. *J Neurol Neurosurg Psychiatry* (2001) 71:285–8. doi:10.1136/jnnp.71.3.285

69. van Gaalen J, Pennings RJ, Beynon AJ, Münchau A, Bloem BR, van de Warrenburg BP. Cervical dystonia after ear surgery. *Parkinsonism Relat Disord* (2012) 18:669–71. doi:10.1016/j.parkreldis.2011.10.004

70. Çoban K, Kansu L, Aydın E. Benign paroxysmal positional vertigo diagnosed in a patient with idiopathic cervical dystonia. *J Clin Pract Res* (2018) 40:42–4. doi:10.5152/etd.2018.17058

71. Li J, Kim S, Pappas SS, Dauer WT. CNS critical periods: implications for dystonia and other neurodevelopmental disorders. *JCI Insight* (2021) 6:e142483. doi:10.1172/jci.insight.142483

72. Li J, Levin DS, Kim AJ, Pappas SS, Dauer WT. TorsinA restoration in a mouse model identifies a critical therapeutic window for DYT1 dystonia. *J Clin Invest* (2021) 131:e139606. doi:10.1172/jci139606

73. Maltese M, Stanic J, Tassone A, Sciamanna G, Ponterio G, Vanni V, et al. Early structural and functional plasticity alterations in a susceptibility period of DYT1 dystonia mouse striatum. *Elife* (2018) 7. doi:10.7554/eLife.33331